

Preparation and characterization of Z-type hexaferrites, $\text{Ba}_{3(1-x)}\text{Sr}_{3x}\text{Co}_2\text{Fe}_{24}\text{O}_{41}$ with $x = 0\text{--}0.5$, via a two-step calcination with an intermediate wet milling

M. Aoyama · J. Temuujin · M. Senna · T. Masuko ·
C. Ando · H. Kishi

© Springer Science + Business Media, LLC 2006

Abstract Z-type hexaferrites ($\text{Ba}_{3(1-x)}\text{Sr}_{3x}\text{Co}_2\text{Fe}_{24}\text{O}_{41}$ with $x = 0\text{--}0.5$, Z-hex) were prepared in a nearly phase pure state by a two-step calcination with an intermediate wet milling. The first calcination of the starting mixture comprising oxides or hydroxides at temperatures below 1100°C brought about a mixture of layer-structured M and Y-type hexaferrite phases, together with a spinel phase of Co ferrite. Z-hex was fully crystallized after the second calcination up to 1230°C . Wet milling between the two calcination steps was decisive for the phase purity. Emphasis was laid on the quantitative analyses of Z-hex, together with the evaluation of anisotropic growth of the crystallites. Sr addition stabilizes Z-hex, while decreases degree of anisotropy simultaneously.

Keywords Ba hexaferrites · Z-phase, preparation of · Wet milling · Particle morphology · Anisotropic grain growth

1 Introduction

Development of wireless telecommunication technology, notably wireless LAN system, ever requires higher frequency, exceeding 1 GHz. Magnetic permeability fade at these high frequency is, therefore, a serious problem for materials en-

gineers. From these requirements, hexagonal ferrites gathers increasing interests, since they are expected to absorb high frequency noises [1, 2].

Z-type hexagonal barium ferrite (Z-hex) is one of the hexagonal ferrites and has rather high permeability up to the GHz region, and hence much superior than conventional spinel ferrites [3]. However, it is not easy to synthesize phase pure Z-hex because of its complex structure. Z-hex is regarded as a sum of M- ($\text{BaFe}_{12}\text{O}_{19}$; M-hex) and Y- ($\text{Ba}_2\text{Co}_2\text{Fe}_{12}\text{O}_{22}$; Y-hex) type ferrites, and, hence, more complicated than its constituents. The structure contains 33 close-packed layers, stacked along the hexagonal *c*-axis, and ordered in units called S, R, T blocks [4].

There are some reports on the synthesis of Z-hex. Among various chemical synthesis techniques, citrate precursors [5] and sol-gel method [6, 7] have been proven to be effective in reducing the sintering temperature and achieving desirable properties.

By a conventional ceramic route, the phase formation and sintering temperature of Z-hex is higher than 1300°C . For the solid-state synthesis of Z-hex, topotactic growth from the mixture of M-hex and Y-hex is involved, with the appropriate restacking of the layer units. We, therefore, may expect a more rational solid-state reaction toward Z-hex from subsequent heating if we obtained intimate mixtures comprising M-hex and Y-hex mixed phases with their particle size small enough to minimize the diffusion paths toward the full crystallization of Z-hex. For this purpose, we suppose the wet milling to be superior over dry milling in reducing particle size while keeping the crystallinity high enough. We obtained phase pure Z-hex at 1230°C and confirmed the effects of wet milling condition on the Z-hex crystallization [8].

To further reduce the reaction temperature and particle size, we ground raw materials before the first calcination, to

M. Aoyama · J. Temuujin · M. Senna (✉)
Department of Applied Chemistry, Faculty of Science and
Technology, Keio University, 3-14-1, Hiyoshi, Yokohama-shi
223-8522
e-mail: senna@applc.keio.ac.jp

T. Masuko · C. Ando · H. Kishi
Materials Research and Development Division, General Research
and Development Laboratories, Taiyo Yuden Co. Ltd., 5607-2
Nakamuroda, Gunma 370-3347

expect mechanochemical effects on the raw materials with simultaneous reduction of particle size. We also pay attention to exactly analyze the phase purity and its preferred orientation of Z-hex.

2 Experimental

2.1 Materials

Raw materials used were analytical grade reagents BaCO_3 , SrCO_3 , $\alpha\text{-FeOOH}$, Co_3O_4 and Co(OH)_2 we used them as purchased. A stoichiometric mixture for Z-hex composition, by using BaCO_3 (as barium source), SrCO_3 (as strontium source), $\alpha\text{-Fe}_2\text{O}_3$ or FeOOH (as iron source), and Co_3O_4 or Co(OH)_2 (as cobalt source), was prepared by milling in water in a conventional rotational ball mill with ZrO_2 balls for 2 h, and dried at 100°C for 12 h.

A part of the stoichiometric mixture was subjected to milling by a planetary ball mill (Fritsch, Pulverisette 5) for mechanical activation, for 1 h in a 250 ml corundum pot with a nylon-coated iron balls at 250 rpm/70 rpm (rotation/revolution). The weight ratio of the balls to the powder was kept constant at 50:1. Details of wet and dry milling conditions are given elsewhere [8]. The starting mixtures were calcined at 1080°C for 2 h to obtain intermediates. Three grams of the intermediate were dispersed in 50 ml distilled water and milled with planetary mill for 1 h in a 250 ml corundum pot with nylon-coated iron balls under the same conditions given above. The slurry was dried at 50°C for 48 h and subsequently calcined again at 1230°C for 2 h.

2.2 Characterization

Crystalline phases were characterized by powder X-ray diffractometry (XRD, Model No. RINT-2000, Rigaku). Particle morphology was observed by a field emission scanning electron microscope (FE-SEM, Hitachi, S-4000).

3 Results and discussion

3.1 Phase composition of the calcined products

As shown in Fig. 1, we have obtained fairly well crystallized Z-hex, regardless of whether we added Sr or not. The relative intensity of the diffraction peaks is, however, quite different. At a sight, the sample SZ-1080-1-1230 is by far closer to the JCPDS—registered data given at the bottom. However, we have to pay attention to the effect of preferred orientation. In order to rationally analyze the phase composition and the degree of preferred orientation, we paid efforts to separate the

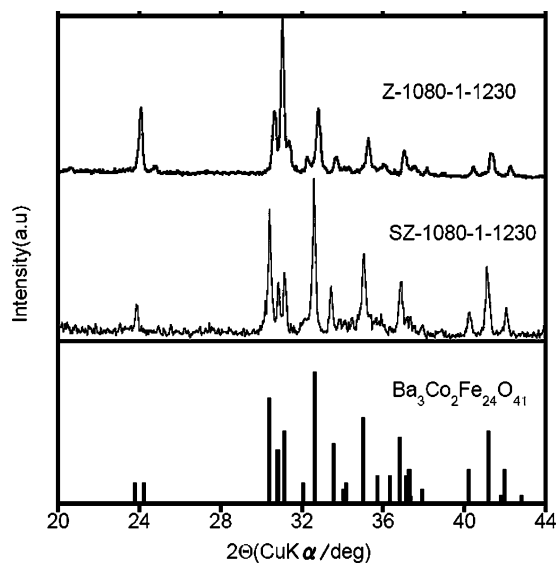


Fig. 1 XRD patterns of samples Z-hex

diffraction peaks and tried to evaluate the percent of Z-hex from all the crystalline parts by using Eq. (1):

$$Z(\%) = \frac{\sum IZ(\text{without preferred orientation})}{\sum IZ(\text{without preferred orientation}) + \sum IM, Y, Z} \quad (1)$$

where IZ (without preferred orientation) includes the intensity of the diffraction peaks of Z(110), (114), (116) and (101 $\bar{6}$), but excludes those of (00 l).

Once the peaks from the Z-hex were well identified, then the degree of preferred orientation, $L(00l)$ with respect to (00 l) was evaluated from Lotgering's equation:

$$L(00l) = \frac{\sum IZ(00l) \sum IZ(\text{all}) - \sum IZ_0(00l) \sum IZ_0(\text{all})}{1 - \sum IZ_0(00l) \sum IZ_0(\text{all})} \quad (2)$$

where IZ_0 is the diffraction intensities, IZ , for a randomly oriented powder specimen, from the JCPDS.

Thus, we obtained the values given in Table 1 from the diffractograms given in Fig. 1. While the percent Z phase is higher by incorporating Sr ($x = 0.5$), significant preferred orientation takes place in the sample without Sr-doping. We attribute the latter to the difference of the ionic radius of Ba and Sr to change the site distribution and to induce the anisotropic distribution of Co.

3.2 Effect of mechanical treatment on the starting mixture

Effects of mechanical activation of the starting mixture were examined. As shown in Fig. 2, we observe differences between the samples with or without mechanical treatment

Table 1 Crystallographical analyses of Z-hex

	Preparation condition			Percent of Z phase Z (%)	Degree of orientation L(001)
	A*	B*	C*		
Sr/Ba	1080	1	1230	91	2
Ba	1080	1	1230	71	47

*A: 1. calcination temperature (°C), B: Milling time (h), C: 2. calcination temperature (°C).

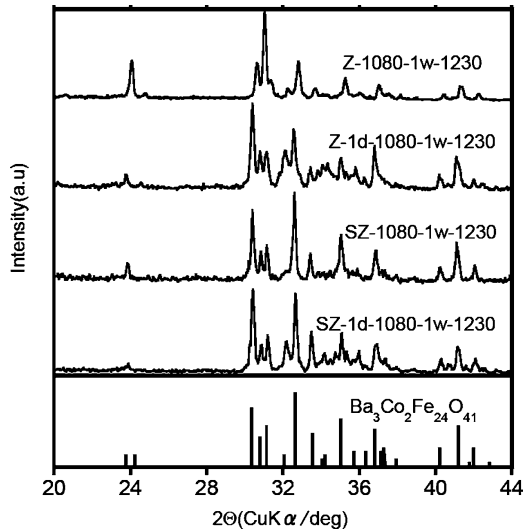


Fig. 2 XRD patterns of samples Z-hex with or without mechanical processes in starting mixture

on the starting mixture. Samples from the mechanically treated starting mixture contain mainly Z-hex but also Y-hex, W-hex ($\text{BaCo}_2\text{Fe}_{16}\text{O}_{27}$) and some unknown phases. W-hex appears at 1230°C , the peaks at $2\theta = 30.272^\circ$ and 32.053° , corresponding to W(110) and W(114) respectively. W-hex was not observed in samples started from the starting mixture without mechanical treatment. Regardless of Sr-doping, Z-phase content was much higher by starting from the samples with mechanical treatment, i.e., 79% and 95%, respectively.

From the shape of XRD profiles, there was no indication of the orientation of Z-hex with mechanical treatment. The full width at half maximum (FWHM) of Z(110) and Z(0018) are shown in Table 2.

These results indicate that mechanical activation on the raw materials suppresses the crystal growth but promotes

phase transitions. Z-hex is not formed directly from the simple oxides. With gradually increasing the temperature, samples change the phase, starting from ingredient oxides to spinels, M-hex at 800°C , Y-hex at 1000°C , Z-hex at 1250°C and finally to W-hex phase over 1300°C [9, 10]. In the case of the two-step process, the first step calcination brings, in a sequence, about M-hex and Y-hex, while in the second step, Z-hex and finally W-hex. These results demonstrate that the effect of mechanical activation on the starting mixture lasts until the end of the second calcination. By mechanical activation on the starting mixture, the percent of Z phase was improved from 71 to 79% in the sample without Sr-doping, and from 91 to 95% in the Sr-doped sample after the second step calcination.

3.3 Morphological observation

Figure 3 displays SEM micrographs of Z-hex and Sr-doped Z-hex powders with or without mechanical activation on the raw materials. We observe platelet grains to give agglomerates of above $20\ \mu\text{m}$. The particles given in Fig. 3(a) and (c) exhibit their size larger than $5\ \mu\text{m}$, while those with preliminary mechanical activation, given in Fig. 3(b) and (d) were significantly smaller than $5\ \mu\text{m}$. Thus, mechanical activation before the first step calcination reduces the particle size and diffusion paths, and activates raw materials.

4 Conclusion

Z-type hexaferrites ($\text{Ba}_{3(1-x)}\text{Sr}_{3x}\text{Co}_2\text{Fe}_{24}\text{O}_{41}$ with $x = 0-0.5$, Z-hex) were synthesized by a two-step calcination at temperatures as low as 1230°C with an intermediate wet milling. The content of Z-hex was analyzed as quantitatively

Table 2 Full width at half maximum (FWHM) of Z-hex

	Preparation condition				FWHM		Percent of Z phase Z (%)
	A*	B*	C*	D*	Z(110)	Z(0018)	
Ba	–	1080	1	1230	0.188	0.188	71
Ba	1	1080	1	1230	0.294	0.235	79

*A: Milling time (h), B: 1 calcination temperature (°C), C: Milling time (h), D: 2 calcination temperature (°C).

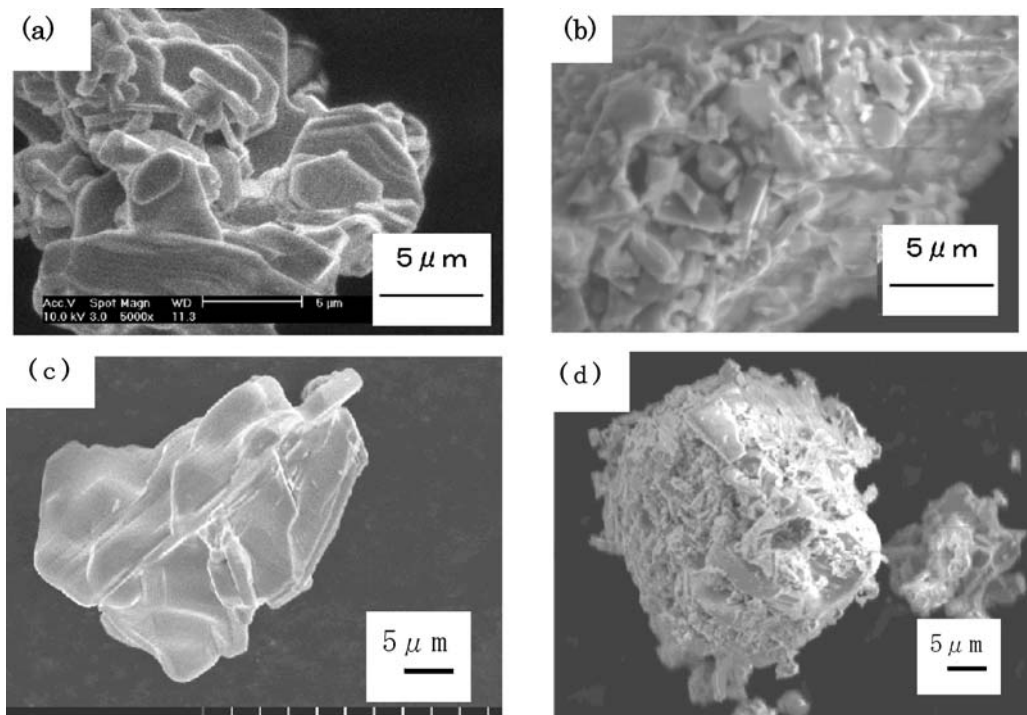


Fig. 3 SEM micrographs of Z-hex calcined. (a) Z without mechanical activation on starting mixture, (b) Z with mechanical activation on starting mixture, (c) SZ without mechanical activation on starting mixture, (d) SZ with mechanical activation on starting mixture

as possible, together with the extent of anisotropic growth of the crystallites. The percent of Z-hex was higher by incorporating Sr while significant preferred orientation took place in the sample without Sr-doping. From XRD studies and SEM micrographs, we found the effect of mechanical treatment on the starting mixture to last until the end of the second calcination. With mechanical activation in the starting mixture, Z phase fraction further increased after second step calcination.

References

1. T. Tachibana, T. Nakagawa, Y. Takada, T. Shimada, and T. Yamamoto, *J. Magn. Magn. Mater.*, **284**, 369 (2004).
2. M. Pardavi-Horvath, *J. Magn. Magn. Mater.*, **215–216**, 171 (2000).
3. O. Sakaguchi, T. Kagotani, D. Book, H. Nakamura, S. Sugimoto, M. Okada, and M. Homma, *Mater. Trans. JIM*, **37**, 878 (1996).
4. H.A. Elkady, M.M. Abou-Sekkina, and K. Nagorny, *Hyperfine Interactions*, **128**, 423 (2000).
5. X. Wang, L. Li, Z. Gui, S. Shu, and J. Zhou, *Mater. Chem. Phys.*, **77**, 248 (2002).
6. G. Xiong, G. Wei, X. Yang, L. Lu, and X. Wang, *J. Mater. Sci.*, **35**, 931 (2000).
7. R.C. Pullar, S.G. Appleton, M.H. Stacey, M.D. Taylor, and A.K. Bhattacharya, *J. Magn. Magn. Mater.*, **186**, 313 (1998).
8. J. Temuujin, M. Aoyama, M. Senna, T. Masuko, C. Ando, and H. Kishi, *J. Mater. Res.*, **20**, 1939 (2005).
9. X. Wang, L. Li, Z. Yue, S. Su, Z. Gui, J. Zhou, *Mater. Chem. Phys.*, **77**, 248 (2002).
10. T. Tachibana, T. Nakagawa, Y. Takada, K. Izumi, T. Yamamoto, T. Shimada, and S. Kawano, *J. Magn. Magn. Mater.*, **262**, 248 (2003).